[CANCER RESEARCH 31, 1977–1989, December 1971]

Acute Ultrastructural Effects of Benzo[a]pyrene and Ferric Oxide on the Hamster Tracheobronchial Epithelium

Curtis C. Harris, Michael B. Sporn, David G. Kaufman, Joseph M. Smith, Mary S. Baker, and Umberto Saffiotti

Lung Cancer Unit, Carcinogenesis, Etiology, National Cancer Institute, NIH, Bethesda, Maryland 20014

SUMMARY

The pathogenesis of epithelial hyperplasia and squamous metaplasia of the tracheobronchial epithelium, induced by polynuclear hydrocarbons, was studied, with the Syrian golden hamster as a suitable animal model. The acute cellular changes in the tracheobronchial epithelium, produced by intratracheal instillations of benzo[*a*]pyrene carried by ferric oxide particles, included focal replacement of the columnar cells with pleomorphic cells. These had the ultrastructural features of atypical squamous cells, *i.e.*, cytoplasmic filaments, widened intercellular spaces, abnormal desmosomes, and increased number of lysosomal derivatives. Polylobulated nuclei and pleomorphic nucleoli were prominent findings after multiple instillations of benzo[*a*]pyrene:ferric oxide. Intratracheal instillations of ferric oxide alone or pyrene:ferric oxide produced basal cell hyperplasia, which was reversible. The atypical squamous cells induced by benzo[*a*]pyrene:ferric oxide had ultrastructural features similar to hyperplastic epithelial cells described in the bronchi of smoking dogs and neoplastic squamous cells described in human bronchogenic carcinoma. This investigation is one of a series of studies to clarify the histogenesis of squamous cell carcinoma of the lung.

INTRODUCTION

The incidence of bronchogenic squamous cell carcinoma in man has shown a progressive increase during the past 5 decades. Experimental animal models for the study of respiratory carcinogenesis have been recently developed and reviewed (26, 27). Saffiotti *et al.* (28) have shown that intratracheal instillation of benzo[*a*]pyrene carried on ferric oxide particles produces squamous metaplasia and squamous cell carcinomas in the respiratory epithelium of the Syrian golden hamster.

The pathogenesis of bronchogenic carcinoma is being studied in this animal model. The most prevalent type of respiratory tumor, in man as well as in this animal model, is squamous cell carcinoma. Therefore, squamous differentiation is an intrinsic component of the most common neoplastic response of the respiratory epithelium. Work in our laboratory is directed at defining the process of squamous differentiation and at understanding the intimate relationships between squamous cell differentiation, metaplasia, and squamous cell cancer. The acute ultrastructural changes produced by benzo[*a*]pyrene and ferric oxide are described in this report. In addition, long-term serial sacrifice studies are in progress to follow the fate of the acute ultrastructural lesions produced by benzo[*a*]pyrene:ferric oxide, up to the time of tumor development.

Received February 25, 1971; accepted July 23, 1971.

MATERIALS AND METHODS

Young adult male Syrian golden hamsters (Lakeview Hamster Colony, Newfield, N. J.) initially weighing 100 to 120 g were maintained on Wayne Lab-Blox diet (Allied Mills, Inc., Chicago, Ill.) and water *ad libitum*. Benzo[*a*]pyrene (more than 98% pure, Aldrich Chemical Company, Inc., Milwaukee, Wis.) and pyrene (more than 98% pure, Eastman Organic Chemicals, Rochester, N. Y.) carried on ferric oxide (Type R8089; particle size, 93% by weight $< 5\ \mu$, 80% $< 2\ \mu$, and 68% $< 1\ \mu$ in diameter; Minerals, Pigments and Metals Division, Pfizer, Inc., New York, N. Y.) were prepared as a 1:1 mixture suspended in sterile 0.9% NaCl solution and administered by intratracheal instillation as previously described (28). Untreated, as well as 0.9% NaCl solution- and sham-treated animals (4 to 8 animals/group at each time period), served as controls. Sodium methohexital (4 mg/animal) dissolved in sterile 0.9% NaCl solution was given by i.p. injection for anesthesia. The treatments and times of sacrifice are listed in Table 1.

Four to 8 animals in each group and time interval were sacrificed by a blow to the head or by injection of sodium methohexital (10 mg i.p.). For histological studies, tissues were fixed in neutral-buffered formalin. The tissues were embedded in paraffin and sections stained with periodic acid:Schiff or hematoxylin and eosin.

For electron microscopy, intact tracheal rings from the upper and lower third of the trachea and bronchial rings from the right mainstem bronchus were fixed in 1.33% osmium tetroxide buffered by 0.1 M *s*-collidine, pH 7.4, dehydrated in a graded series of ethanol, and embedded in Epon 812 containing 5% araldite as previously described (13). One-μ cross-sections of the tracheal rings were stained with toluidine blue (38). Ultrathin sections were cut on an LKB microtome and were stained with aqueous uranyl acetate and lead citrate. The sections were examined in a Phillips 200 electron microscope at 60 kV.

Table 1
Treatment and sacrifice schedule

Treatment[a]	Time of sacrifice (hr) after following no. of instillations[b]		
	1	4	10
Ferric oxide (5 mg)	24, 48, 72	48	48
Pyrene (5 mg) + ferric oxide (5 mg)	24, 48, 72	48	48
Benzo[*a*]pyrene (5 mg) + ferric oxide (5 mg)	24, 48, 72	48	48
0.9% NaCl solution (0.2 ml)	24, 48, 72	48	48
Sham treatment[c]	24, 48, 72	48	48

[a] Agents were suspended in 0.2 ml of 0.9% NaCl solution and instilled intratracheally.
[b] Time of sacrifice is in hr after the last intratracheal instillation. Multiple intratracheal instillations were given on a Monday-Wednesday-Friday schedule each week.
[c] Animals were anesthetized, and 0.2 ml of air was given by intratracheal instillation.

RESULTS

Normal Tracheobronchial Epithelium

The ultrastructure of the tracheobronchial epithelium of the hamster has not been previously described in detail. For the untreated male young adult, the epithelium is columnar (Fig. 1), and the ultrastructure of its ciliated, mucous, and basal cells is similar to that described for these epithelial cells in other animals (5, 8, 25, 39). Briefly, ciliated cells (Fig. 1) are attached to adjacent columnar cells by desmosomes and by tight junctions at the luminal surface. A narrow intercellular space separates the cells. At the cell apex are typical cilia rooted in the cytoplasm by basal bodies. In addition, narrow cytoplasmic processes project into the luminal surface. The nucleus is somewhat irregular in contour and contains a small, round nucleolus with a nucleolonema. Numerous mitochondria, free and membrane-bound ribosomes, and a few filaments are found in the cytoplasm.

In the young adult hamsters observed, mucous or goblet cells (Fig. 1) were not as well developed as those described in the dog (8) or man (25, 39). Large packets of mucous granules are seldom seen. Golgi complexes and mucous granules are observed at the cell apex and stacks of rough endoplasmic reticulum are located primarily in the basal area. Mitochondria are oval or elongated and contain typical horizontal cristae.

Basal cells are polygonal (Fig. 2). They are attached to the basement membrane by hemidesmosomes and to adjacent cells by desmosomes. The intercellular space is narrow, and cytoplasmic interdigitations are present. Free ribosomes, filaments, and, rarely, Golgi complexes are observed in the cytoplasm. A large oval nucleus is centrally located and contains a small nucleolus. Intermediate cells differentiating into mucous or ciliated cells are also observed.

Sham treatment or the intratracheal instillation of 0.9% NaCl solution produced few ultrastructural changes. Intermediate cells lining the lumen were found on 3 occasions following multiple intratracheal instillations of 0.9% NaCl solution (Fig. 3). Some of these cells were occasionally observed to contain filaments within cristae of endoplasmic reticulum (Fig. 4).

Ferric Oxide-treated Tracheobronchial Epithelium

A single intratracheal instillation of ferric oxide produced no ultrastructural lesions. Ten instillations resulted in a widespread focal replacement of the columnar epithelium with polygonal basal cells in all treated animals (Figs. 5 to 7). The luminal cells showed a light cytoplasmic density as compared to the darker cells adjacent to the basement membrane (Fig. 6). These hyperplastic cells contained many cytoplasmic filaments, relatively few organelles, numerous desmosomes, narrow intracellular spaces, and complex interdigitations between cells (Fig. 7). Nuclei and nucleoli were typical of basal cells. An additional group of 4 animals was sacrificed 6 weeks after the last of 10 instillations of ferric oxide. The hyperplastic response was found to have reverted to normal in all 4 animals examined.

Pyrene:Ferric Oxide-treated Tracheobronchial Epithelium

The addition of the noncarcinogenic hydrocarbon, pyrene, to ferric oxide produced histological and ultrastructural alterations similar to those described with ferric oxide alone, including the reversibility of the basal cell hyperplasia, also observed in an additional group of 4 animals sacrificed 6 weeks after the last of 10 treatments.

Benzo[*a*]pyrene:Ferric Oxide-treated Tracheobronchial Epithelium

Single Intratracheal Instillation. By 24 hr, vesiculation of the endoplasmic reticulum, increased numbers of free ribosomes, and occasional cell necrosis were observed in both ciliated and mucous cells (Fig. 8). Nuclei were somewhat enlarged, but nucleoli appeared normal. By 48 hr, a slight increase in number of intermediate cells and widening of intercellular spaces were evident in focal areas. Nuclei and nucleoli were occasionally enlarged (Fig. 9). A further increase of intermediate cells was found at 72 hr (Fig. 10). The intermediate cells contained stacks of rough endoplasmic reticulum and showed an increased nucleus to cytoplasm ratio. The number of desmosomes was decreased. Complex cytoplasmic interdigitations joined cells together.

Multiple Intratracheal Instillations. Four instillations of benzo[*a*]pyrene carried on ferric oxide caused areas of disordered epithelial architecture with focal areas of squamous metaplasia by light microscopy (Fig. 11). When serial sections were examined, decreased numbers of cilia were found (Fig. 12). Lysosomes and degenerating mitochondria were increased in number. Membrane-bound filamentous granules were found in small clusters near the luminal surface of some cells (Fig. 13) and were similar to the "special cell type" granules observed by Frasca *et al.* (8) infrequently in the bronchial epithelium of normal dogs and frequently in smoking dogs (9). These structures may be aberrant internalized cilia, secretory product, or degenerating mitochondria. They were observed

Table 2
Ultrastructural pathology of epithelial hyperplasia and squamous cell carcinoma

	Squamous cell carcinoma in man[a]	Epithelial hyperplasia induced by benzo[a]pyrene ferric oxide in hamsters[b]	Epithelial hyperplasia induced by cigarette smoking in dogs[c]
Intercellular relationships and attachments			
Cellular morphology	Polygonal	Polygonal	Columnar and polygonal
Intercellular space	Widened	Widened	Widened
Desmosomes	Decreased	Decreased, abnormal	Decreased
Nucleus			
Nucleus/cytoplasm	Increased +++[d]	Increased ++	Increased +
Shape	Polylobulated	Polylobulated	Irregular
Nucleoli	Enlarged, pleomorphic	Enlarged, pleomorphic	Enlarged
Cytoplasm			
Tonofilaments	Increased +++, dispersed, and perinuclear bundles	Increased +++, dispersed, and perinuclear bundles	Increased +
Lysosomes	Increased ++	Increased ++	Increased +
Mitochondria	Decreased +++, abnormal	Decreased ++, abnormal	Decreased +, abnormal
Endoplasmic reticulum	Increased smooth ++ Decreased rough +++	Increased smooth ++ Decreased rough ++	Unchanged
Free ribosomes	Increased	Increased	Increased
Other organelles	Internalized cilia, rare	Filamentous granules	Filamentous granules

[a] Refs. 4, 10, 20, 21, 23, 33, and 40.
[b] Present observations.
[c] Ref. 9.
[d] Gradation of change: +++, greatest; ++, moderate; and +, least.

only in the carcinogen-treated epithelium. Nuclei appeared to be enlarged.

Ten instillations of benzo[a]pyrene:ferric oxide produced striking ultrastructural changes which are summarized in Table 2. There was widespread focal squamous metaplasia with areas of cellular atypia (Fig. 14). Epithelial hyperplasia was seen adjacent to some areas of squamous metaplasia (Fig. 14). Cells of varying densities were present in the epithelium (Fig. 15). Ultrastructural observations revealed abnormally wide intercellular spaces. The cells appeared polygonal and lacked any evidence of mucous or ciliated differentiation (Figs. 16 and 17). Desmosomes having filaments that were abnormally long for the tracheal epithelium were found (Figs. 18 and 19). The cytoplasm contained many lysosomes, few mitochondria, and numerous filaments occurring singly or as dense perinuclear bundles (Fig. 20). Filamentous granules, such as those described above (Fig. 13), were frequently seen in large clusters (Fig. 21). Enlarged nuclei were indented by deep cytoplasmic invaginations, giving them a polylobulated appearance (Fig. 22). Nucleoli were also enlarged and pleomorphic when compared to normal nucleoli. Nucleolar plaques or microspherules (Fig. 23) occurred, while other nucleoli were microsegregated (Figs. 24 and 25). Macrosegregation implies the presence of distinct zones composed of pure granules or fibrils, while microsegregation implies compact condensations of the fibrils which are distributed throughout the granular component (35).

The basement membrane was frequently discontinuous, and cytoplasmic processes of the epithelial cells projected into the connective tissue layer (Figs. 26 and 27).

DISCUSSION

Previous studies (19, 27, 28) have shown that the intratracheal instillation of benzo[a]pyrene:ferric oxide produces squamous metaplasia and squamous cell carcinoma in the respiratory epithelium of the Syrian golden hamster. This animal model provides an unique opportunity to study the pathogenesis of squamous cell carcinoma. In this study, the acute ultrastructural effects in the tracheobronchial epithelium produced by single and multiple doses of a carcinogenic polynuclear hydrocarbon, benzo[a]pyrene, were compared to the effects of a noncarcinogenic or weakly carcinogenic hydrocarbon, pyrene, and the carrier dust, ferric oxide.

The ultrastructure of the normal tracheobronchial epithelium of the hamster was found to be similar to that of the rat (5), dog (8), mouse (11), and man (25, 39). Only a few experimental observations of the ultrastructural changes in respiratory tract carcinogenesis have been reported thus far. A preliminary description of tracheal papillomas induced in hamster by the systemic carcinogen, dibutylnitrosamine, has been recently published (1). Dirksen and Crocker (5) have reported the ultrastructural alterations produced by polynuclear hydrocarbons in rat tracheal epithelium maintained in organ culture. Carcinogenic hydrocarbons added to the culture media produced squamous metaplasia with some atypia. The altered cells contained little endoplasmic reticulum, many cytoplasmic filaments, abundant free ribosomes, and increased lysosomal derivatives. Nuclei were irregular in contour, and some "fragmentation" of nucleoli was noted. The acute *in vivo* effects of benzo[a]pyrene:ferric oxide on tracheobronchial epithelium are in some ways similar to the *in vitro* effects reported by Dirksen and Crocker (5). The acute changes observed here *in vivo* are more pronounced and advanced. The intratracheal administration of benzo[a]pyrene:ferric oxide causes enlarged nuclei containing deep cytoplasmic invaginations. The lesions in the nucleus and nucleolus produced by benzo[a]pyrene are of particular interest. Aberrant nuclear and nucleolar morphology remains

an important criterion in the cytological diagnosis of cancer in man. Benzo[*a*]pyrene:ferric oxide produced nucleolar segregation (Figs. 24 and 25) and nucleolar plaques or microspherules (Fig. 23). Nucleolar segregation has been produced by several agents and is not specific for carcinogens (3, 12, 31). This ultrastructural lesion may be reversible and has a temporal association with inhibition of RNA polymerase and RNA synthesis (24).

Tracheobronchial epithelium treated with benzo[*a*]pyrene:ferric oxide (Figs. 14 to 27) acquires many of the ultrastructural characteristics that were observed in hyperplastic epithelium induced by tobacco smoke (9), bronchial carcinoma *in situ* (40), and squamous cell carcinoma of the lung (4, 10, 20, 21, 23, 33). Table 2 summarizes these comparisons. The morphological similarities between atypical metaplastic squamous cells caused by benzo[*a*]pyrene:ferric oxide and frank neoplastic squamous cells are not surprising, since squamous metaplasia can be a stage in the tumorigenesis of squamous cell carcinoma in man (2) and this animal model (27, 28).

Studies of other epithelia during tumorigenesis have shown ultrastructural changes similar to those described here. Tarin (36) described the sequential changes in mouse skin carcinogenesis caused by methylcholanthrene and concluded, "The principal alterations in the epidermis consist of hyperplasia, loss of contact between basal cells, pleomorphism and disturbance of cellular arrangement." Widened intercellular spaces, decreased number of desmosomes, and nexus deficiency have also been observed in squamous cell carcinoma of the human cervix (30). McNutt *et al.* (18) have also described these changes in preinvasive lesions of the cervical epithelium, *i.e.*, severe dysplasia and carcinoma *in situ*. Finally, the epithelium of the colon undergoes ultrastructural changes in the initial stages of tumorigenesis that are similar to those described above (7, 14, 32).

Tarin (37) has discussed the possible significance of the ultrastructural changes at the epithelio-mesenchymal junction during carcinogenesis. Fragmentation of the basement membrane and microinvasion into the connective tissue layer by epithelial processes has been described in premalignant and malignant lesions of the skin (36), mammary gland (22, 37), and the larynx (34). Similar changes in the tracheobronchial epithelium were found following cigarette smoking (9) and in this investigation (Figs. 26 and 27).

Multiple intratracheal doses of ferric oxide dust or pyrene:ferric oxide produced a marked basal cell hyperplasia (Figs. 5, 6, and 7), which was reversible. This hyperplastic response induced by ferric oxide may play an important role in the mechanism of respiratory carcinogenesis in this animal model, since intratracheal administration of benzo[*a*]pyrene in 0.9% NaCl solution without ferric oxide has failed thus far to induce tumors (15, 16, 29). While intratracheal instillation of ferric oxide alone does not cause tumors in hamsters, the incidence of peripheral lung tumors induced by diethylnitrosamine is markedly increased by subsequent multiple intratracheal administration of ferric oxide (19). Hematite miners have an increased incidence of lung cancer (6, 17).

REFERENCES

1. Althoff, J., and Wilson, R. Morphological Changes in the Respiratory System of Syrian Golden Hamsters after Treatment with Dibutylnitrosamine. *In:* P. Nettesheim, M. Hanna, and J. Deatherage (eds.), Morphology of Experimental Respiratory Carcinogenesis, Atomic Energy Commission Symposium, Ser. 21, pp. 359–364. Springfield, Va.: National Technical Information Service, U. S. Department of Commerce, 1970.
2. Auerbach, O., Stout, A., Hammond, E., and Garfinkel, L. Changes in Bronchial Epithelium in Relation to Lung Cancer. New Engl. J. Med., *265:* 253–259, 1961.
3. Busch, H., and Smetana, K. The Nucleolus, pp. 472–501. New York: Academic Press, Inc., 1970.
4. Coalson, J., Mohr, J., Pirtle, J., Dee, A., and Rhoades, E. Electron Microscopy of Neoplasms in the Lung with Special Emphasis on the Alveolar Cell Carcinoma. Am. Rev. Respirat. Dis., *101:* 181–197, 1970.
5. Dirksen, E., and Crocker, T. Ultrastructural Alterations Produced by Polycyclic Aromatic Hydrocarbons on Rat Tracheal Epithelium in Organ Culture. Cancer Res., *28:* 906–923, 1968.
6. Faulds, J. Hematite Pneumoconiosis in Cumberland Miners. J. Clin. Pathol., *10:* 187–199, 1957.
7. Fisher, E., and Sharkey, D. The Ultrastrucutre of Colonic Polyps and Cancer with Special Reference to the Epithelial Inclusion Bodies of Leuchtenberger. Cancer, *15:* 160–170, 1962.
8. Frasca, J., Auerbach, O., Parks, V., and Jamieson, J. Electron Microscopic Observations of the Bronchial Epithelium of Dogs. I. Control Dogs. Exptl. Mol. Pathol., *9:* 363–379, 1968.
9. Frasca, J., Auerbach, O., Parks, V., and Jamieson, J. Electron Microscopic Observations of the Bronchial Epithelium of Dogs. II. Smoking Dogs. Exptl. Mol. Pathol., *9:* 380–399, 1968.
10. Greene, J., Brown, A., and Divertie, M. Fine Structure of Squamous Cell Carcinoma of the Lung. Mayo Clin. Proc., *44:* 85–95, 1969.
11. Hansell, M., and Moretti, R. Ultrastructure of the Mouse Tracheal Epithelium. J. Morphol., *128:* 159–165, 1969.
12. Harris, C., Grady, H., and Svoboda, D. Alterations in Pancreatic and Hepatic Ultrastructure following Acute Cycloheximide Intoxication. J. Ultrastruct. Res., *22:* 240–251, 1968.
13. Harris, C., Grady, H., and Svoboda, D. Segregation of the Nucleolus Produced by Anthramycin. Cancer Res., *28:* 81–90, 1968.
14. Imal, H., Saito, S., and Stein, A. Ultrastructure of Adenomatous Polyps and Villous Adenomas of the Large Intestine. Gastroenterology, *48:* 188–197, 1965.
15. Kuschner, M. The J. Burns Amberson Lecture: The Causes of Lung Cancer. Am. Rev. Respirat. Dis., *98:* 573–590, 1968.
16. Laskin, S., Kuschner, M., and Drew, R. Studies in Pulmonary Carcinogenesis. *In:* M. Hanna, P. Nettesheim, and J. Gilbert, (eds.), Inhalation Carcinogenesis, Atomic Energy Commission Symposium, Ser. 18, pp. 321–351. Springfield, Va.: National Technical Information Service, U. S. Department of Commerce, 1970..
17. Levin, M. L., Krans, A., Goldberg, I., and Gerhardt, P. Problems in Study of Occupation and Smoking in Relation to Lung Cancer. Cancer, *8:* 932–936, 1955.
18. McNutt, N., Hershberg, R., and Weinstein, R. Nexus Deficiency in Preinvasive Malignant Human Cervical Epithelium. J. Cell Biol., *47:* 135a, 1970.
19. Montesano, R., Saffiotti, U., and Shubik, P. The Role of Topical and Systemic Factors in Experimental Respiratory Carcinogenesis. *In:* M. Hanna, P. Nettesheim, and J. Gilbert (eds.), Inhalation Carcinogenesis, Atomic Energy Commission Symposium, Ser. 18,

pp. 353–371. Springfield, Va.: National Technical Information Service, U. S. Department of Commerce, 1970.

20. Nagaishi, C., Okada, Y., Diado, S., Genka, K., Ikeda, S., and Kitano, M. Electron Microscopic Observations of the Human Lung Cancer. Exptl. Med. Surg., *28:* 177–202, 1965
21. Obiditsch-Mayer, I., and Breitfellner, G. Electron Microscopy in Cancer of the Lung. Cancer, *21:* 945–951, 1968.
22. Ozzello, L., and Sanpitak, P. Epithelial-Stromal Junction of Intraductal Carcinoma of the Breast. Cancer, *26:* 1186–1198, 1970.
23. Razzuk, M., Race, G., Lynn, J., Martin, J., Urschel, H., and Paulson, D. Observations on Ultrastructural Morphology of Bronchogenic Carcinoma. J. Thoracic Cardiovas. Surg., *59:* 581–587, 1970.
24. Reddy, J., and Svoboda, D. The Relationship of Nucleolar Segregation to Ribonucleic Acid Synthesis following the Administration of Selected Hepatocarcinogens. Lab. Invest., *19:* 132–145, 1968.
25. Rhodin, J. The Ultrastructure and Function of the Human Tracheal Mucosa. Am. Rev. Respirat. Dis., *93:* 1–15, 1966.
26. Saffiotti, U. Experimental Respiratory Tract Carcinogenesis. Progr. Exptl. Tumor Res., *11:* 302–333, 1969.
27. Saffiotti, U. Experimental Respiratory Tract Carcinogenesis and Its Relation to Inhalation Exposures. *In:* M. Hanna, P. Nettesheim, and J. Gilbert (eds.), Inhalation Carcinogenesis, Atomic Energy Commission Symposium, Ser. 18, pp. 27–54. Springfield, Va.: National Technical Information Service, U. S. Department of Commerce, 1970.
28. Saffiotti, U., Cefis, F., and Kolb, L. A Method for the Experimental Induction of Bronchogenic Carcinoma. Cancer Res., *28:* 104–124, 1968.
29. Saffiotti, U., Cefis, F., Kolb, H., and Shubik, P. Experimental Studies of the Conditions of Exposure to Carcinogens of Lung Cancer Induction. J. Air Pollution Control Assoc., *15:* 23–25, 1965.
30. Shingleton, H., Richart, R., Wiener, J., and Spiro, D. Human Cervical Intraepithelial Neoplasia: Fine Structure of Dysplasia and Carcinoma *in Situ*. Cancer Res., *28:* 695–706, 1968.
31. Simard, R., and Bernhard, W. The Phenomenon of Nucleolar Segregation: Specific Action of Certain Antimetabolites. Intern. J. Cancer, *1:* 463–479, 1966.
32. Spjut, H., and Smith, M. A Comparative Electron Microscopic Study of Human and Rat Colonic Polyps and Carcinomas. Exptl. Mol. Pathol., *6:* 11–24, 1967.
33. Stoebner, P., Cussac, Y., Porte, A., and LeGal, Y. Ultrastructure of Anaplastic Bronchial Carcinomas. Cancer, *20:* 286–294, 1967.
34. Sugar, J. A Gege Praecancerosisok Es Rakok Korszovettana. Magy. Onkol., *13:* 201–209, 1969.
35. Svoboda, D. J., and Higginson, J. A Comparison of Ultrastructural Changes in Rat Liver due to Chemical Carcinogens. Cancer Res., *28:* 1703–1733, 1968.
36. Tarin, D. Sequential Electron Microscopical Study of Experimental Mouse Skin Carcinogenesis. Intern. J. Cancer, *2:* 195–211, 1967.
37. Tarin, D. Fine Structure of Murine Mammary Tumours: The Relationship between Epithelium and Connective Tissue in Neoplasms Induced by Various Agents. Brit. J. Cancer, *21:* 417–425, 1969.
38. Trump, B., Smuckler, E., and Benditt, E. A Method for Staining Epoxy Sections for Light Microscopy. J. Ultrastruct. Res., *5:* 343–348, 1961.
39. Watson, J., and Brinkman, G. Electron Microscopy of the Epithelial Cells of Normal and Bronchitic Human Bronchus. Am. Rev. Respirat. Dis., *90:* 851–862, 1964.
40. Watson, J., Bryant, V., and Brinkman, G. The Ultrastructure of Epithelium of Human Bronchus in Epidermoid Carcinoma. *In:* R. Uyeda (ed.), Sixth International Congress for Electron Microscopy, pp. 759–760. Tokyo: Maruzen Co. Ltd., 1966.

Fig. 1. Normal tracheal epithelium. Mucous and ciliated cells are separated by a narrow intercellular space. These columnar cells have small nucleoli (*n*). × 4,180.

Fig. 2. Normal tracheal epithelium. Basal cell is adjacent to the thin amorphous basement membrane (*arrow*) and adjoined to columnar cells by desmosomes (*d*). A large nucleus has a small, round nucleolus (*N*). Fine filaments (*F*) encircle the nucleus. × 11,800.

Fig. 3. Tracheal epithelium following 10 intratracheal instillations of 0.9% NaCl solution. Focal areas are found containing basal cells (*B*) and intermediate cells (*I*). *G*, Golgi apparatus. × 5,200.

Fig. 4. Tracheal epithelium following 10 intratracheal instillations of 0.9% NaCl solution. Cristae of smooth endoplasmic reticulum containing filamentous structures in an intermediate cell. × 16,000. *Inset*, higher magnification of filaments. × 30,700.

Fig. 5. Tracheal epithelium following 10 intratracheal instillations of ferric oxide. Epithelial hyperplasia. H & E, × 600.

Fig. 6. Tracheal epithelium following 10 intratracheal instillations of ferric oxide. Basal cell hyperplasia. × 3,960.

Fig. 7. Tracheal epithelium following 10 intratracheal instillations of ferric oxide. Complex interdigitations, narrow intercellular spaces, and numerous desmosomes characterize the intercellular relationships between these cells. Many fine filaments are free in the cytoplasm. × 29,000.

Fig. 8. Tracheal epithelium 24 hr following 1 intratracheal instillation of benzo[*a*]pyrene plus ferric oxide. Degenerating ciliated cell (*D*) is being sloughed, and adjacent ciliated cell has normal nucleoli (*n*) and many small vesicles of endoplasmic reticulum. × 7,900.

Fig. 9. Tracheal epithelium 48 hr following 1 intratracheal instillation of benzo[*a*]pyrene plus ferric oxide. Nucleoli (*n*) appear to be enlarged in some cells. Rough endoplasmic reticulum (*R*) is dilated. × 4,100.

Fig. 10. Tracheal epithelium 72 hr following 1 intratracheal instillation of benzo[*a*]pyrene plus ferric oxide. The epithelium contains several intermediate cells (*I*). × 4,000.

Fig. 11. Tracheal epithelium 48 hr following 4 intratracheal instillations of benzo[*a*]pyrene plus ferric oxide. Disordered epithelial architecture with focal areas of flat squamous cells. H & E, × 400.

Fig. 12. Tracheal epithelium 48 hr following 4 intratracheal instillations of benzo[*a*]pyrene plus ferric oxide. Ciliated cells have slender cytoplasmic processes (*P*) and few cilia (*C*). Many small vesicles and lysosomes (*L*) are found in the cytoplasm. × 4,900.

Fig. 13. Tracheal epithelium 48 hr following 4 intratracheal instillations of benzo[*a*]pyrene plus ferric oxide. Cytoplasm of mucous cells contains several filamentous granules (*arrows*). × 15,300.

Figs. 14 to 27. Tracheal epithelium 48 hr following 10 intratracheal instillations of benzo[*a*]pyrene plus ferric oxide.

Fig. 14. Keratinizing squamous metaplasia adjacent to hyperplastic epithelium (*arrow*). H & E, × 620.

Fig. 15. Epithelial hyperplasia. Cells of varying density are observed. One-μ Epon-embedded sections stained with toluidine blue. × 400.

Fig. 16. Outer layer of undifferentiated cells containing large nuclei. × 2,000.

Fig. 17. Intercellular spaces (*S*) are wide, and few desmosomes adjoin these cells. Nuclei are enlarged and have an irregular contour. × 1,900.

Fig. 18. Wide intercellular space (*S*) and desmosome with abnormally long filaments (*F*). × 42,750.

Fig. 19. Filaments (*F*) from desmosomes join filaments surrounding nucleus (*N*). × 30,700.

Fig. 20. Nucleus is surrounded by dense filaments (*F*) and indented by deep cytoplasmic invaginations (*I*). × 13,700.

Fig. 21. Clusters of filamentous granules in the cytoplasm. × 2,900

Fig. 22. Polylobulated nucleus containing multiple nucleoli (*N*). × 4,900.

Fig. 23. Numerous nucleolar plaques (*arrows*) are found in this enlarged nucleolus. × 13,700.

Fig. 24. Microsegregated nucleolus is shown with increased number of granules (*G*) and focal collections of fibrils (*F*). Centriole (*arrows*) is present in the cytoplasm. × 10,900.

Fig. 25. Fibrils (*F*) are segregated from nucleolar granules (*G*). × 11,800.

Figs. 26 and 27. Basement membrane is discontinuous and cytoplasmic processes of the epithelial cells invade the connective tissue layer. × 18,000 and 16,200, respectively.

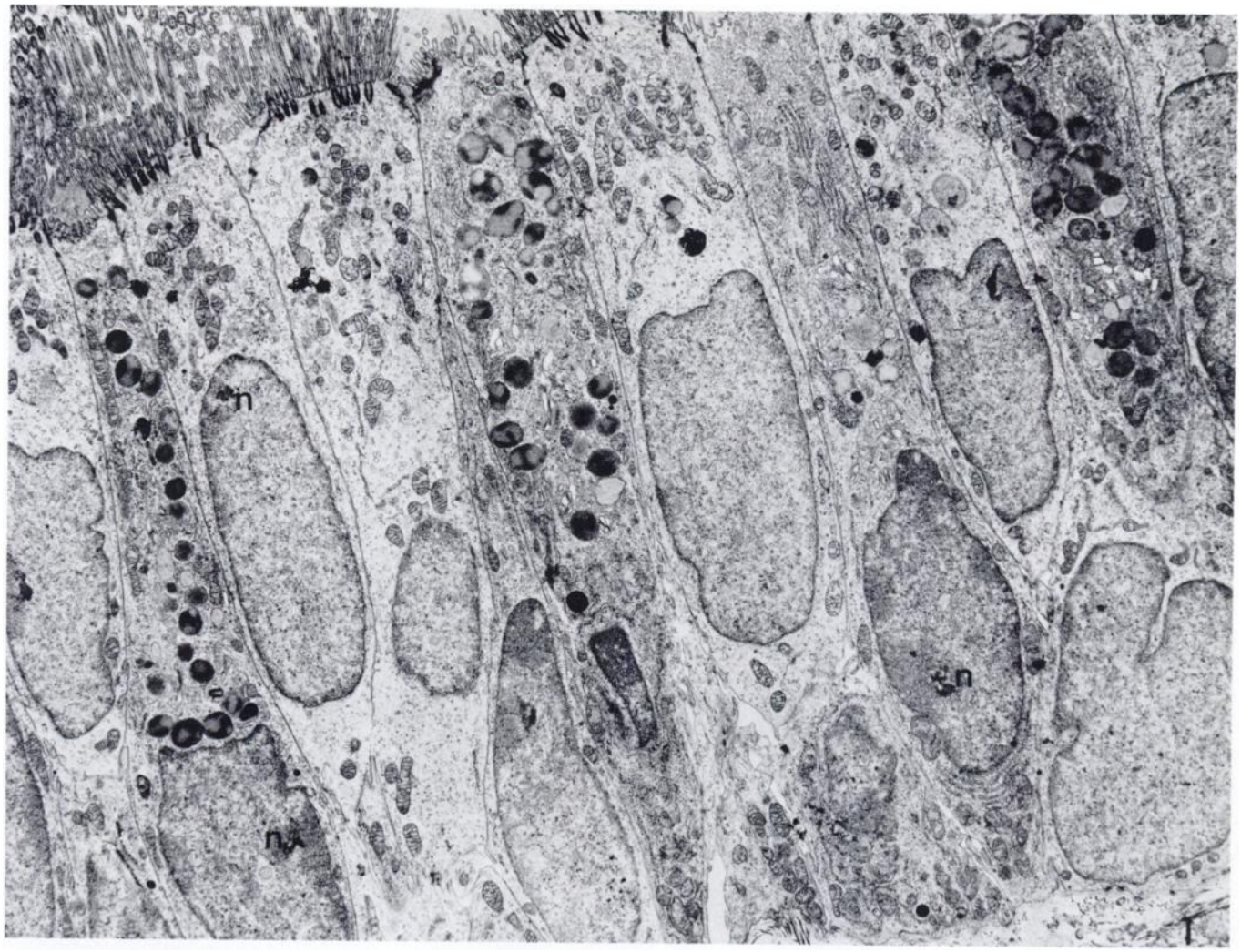

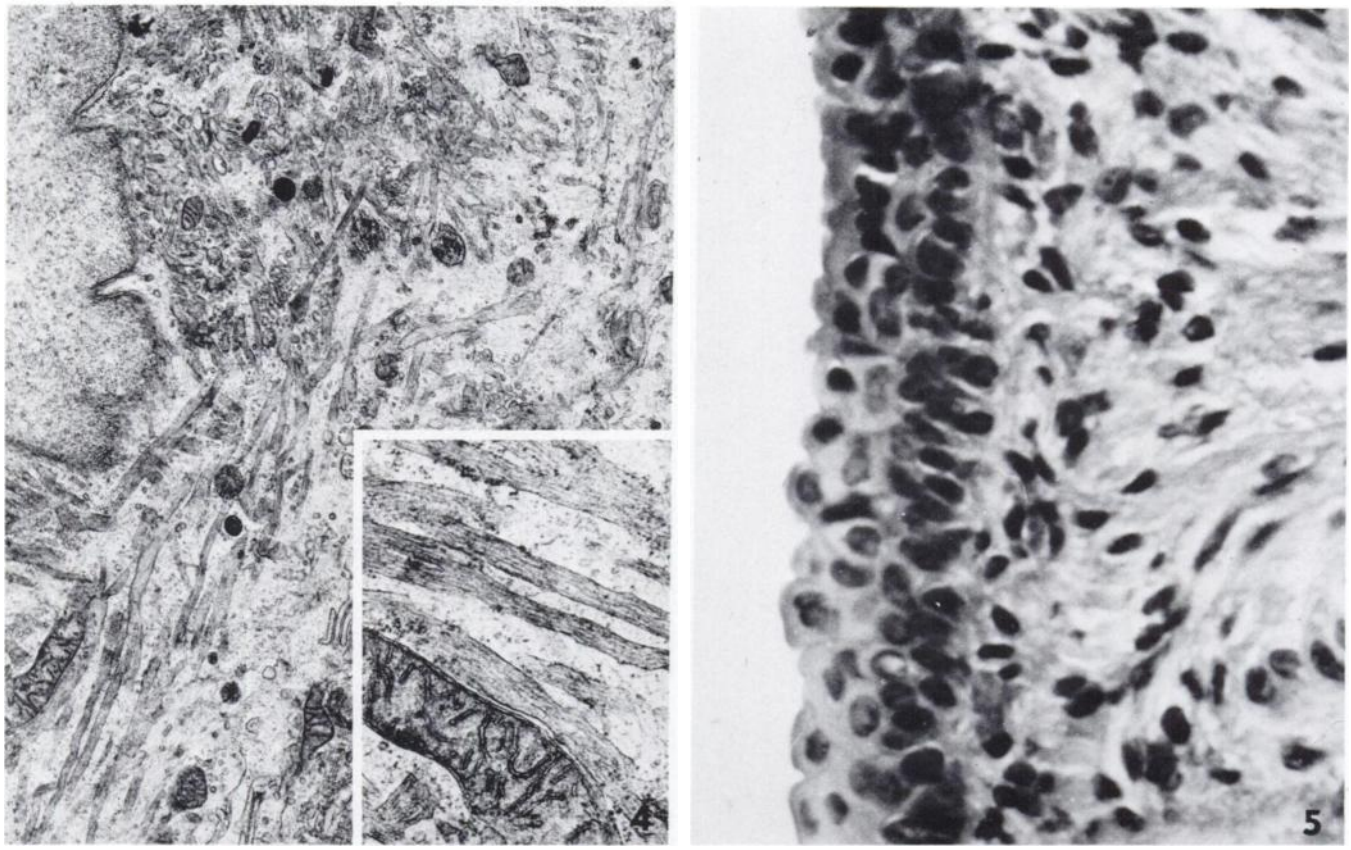

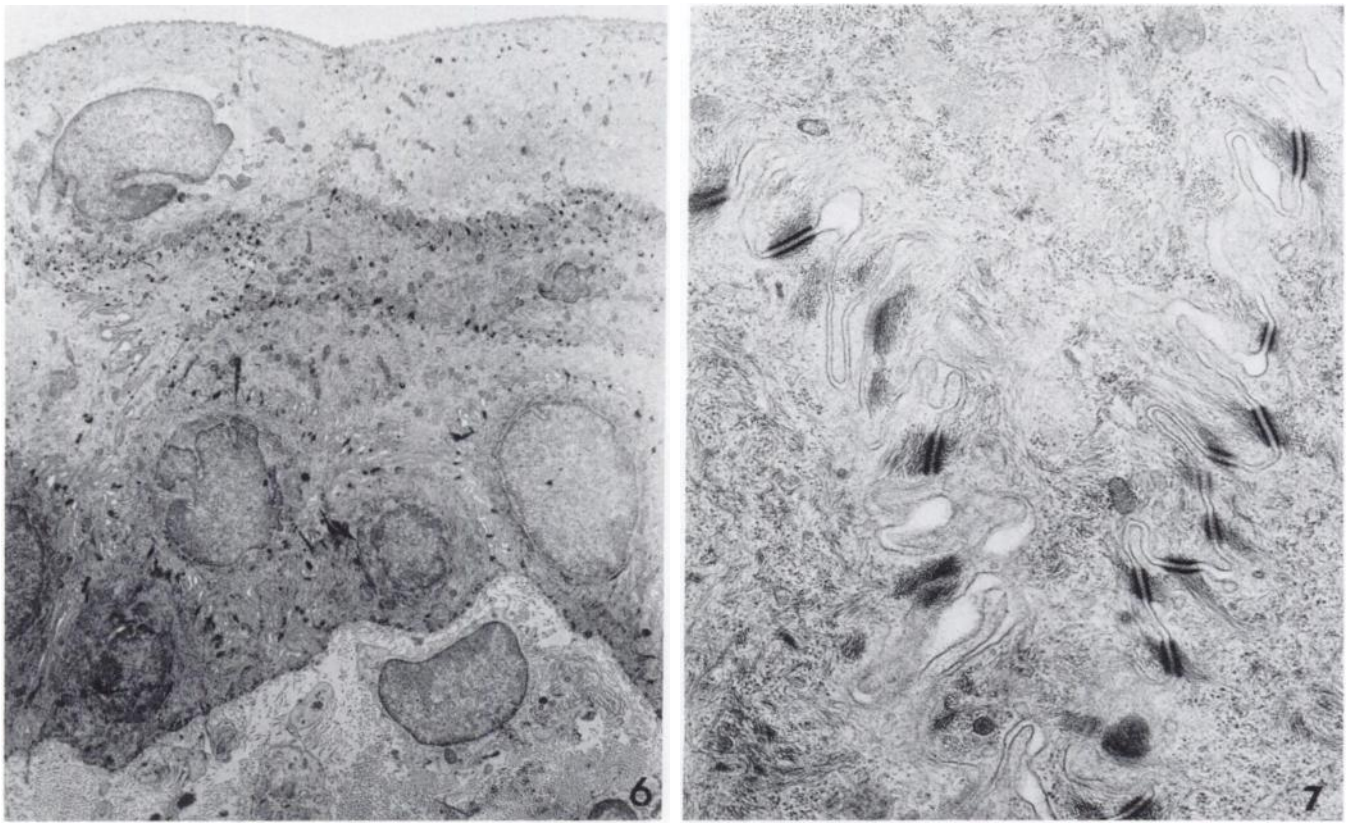

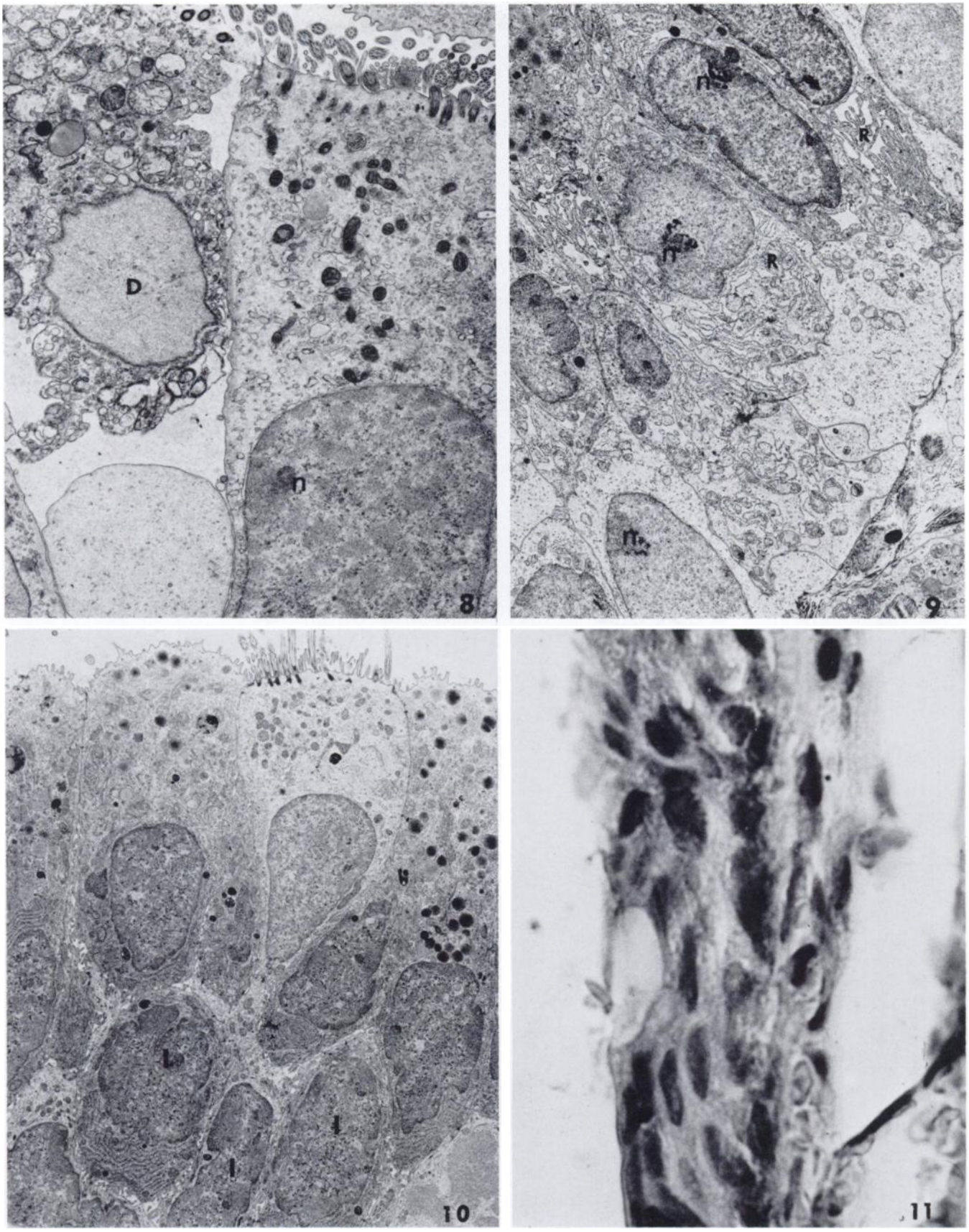

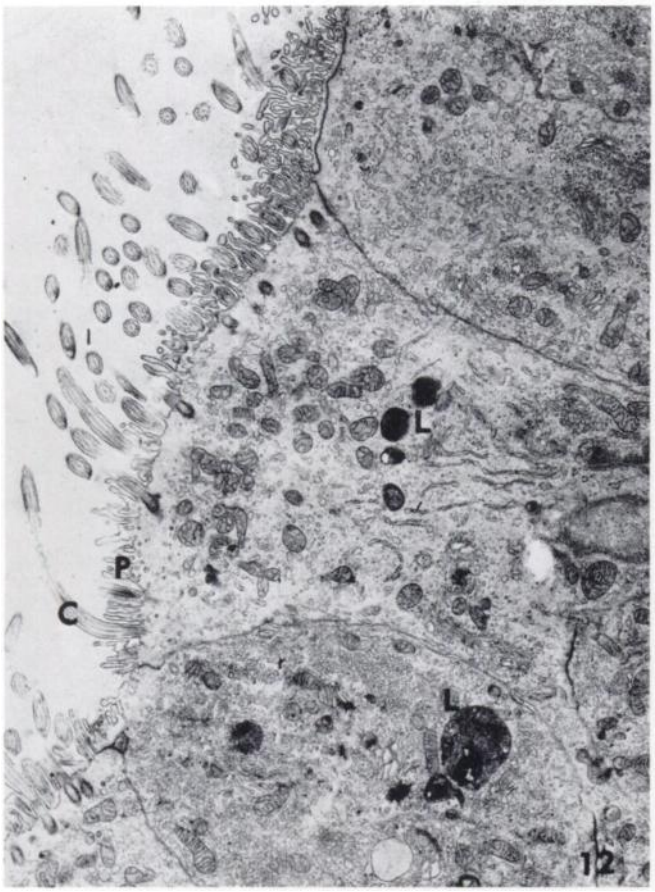

12

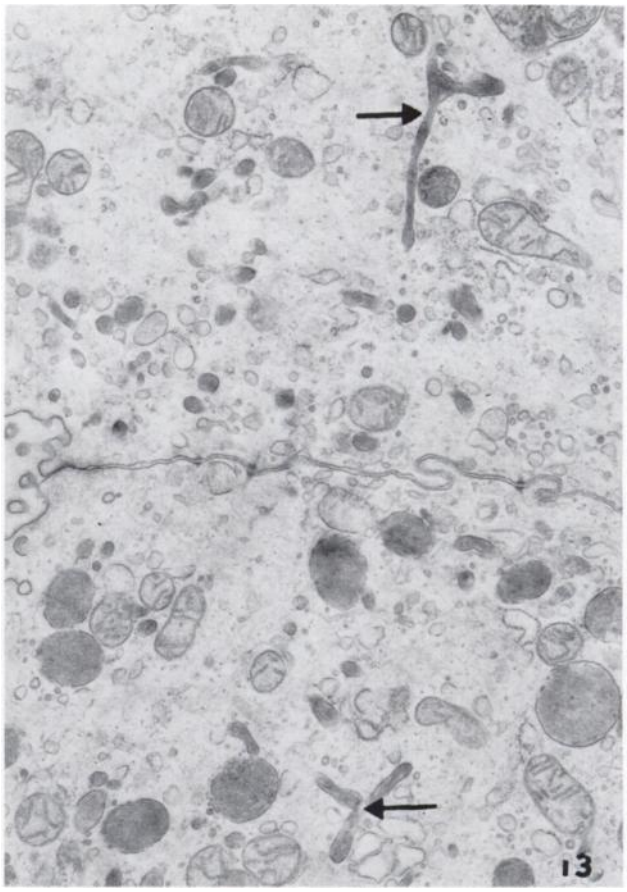

13

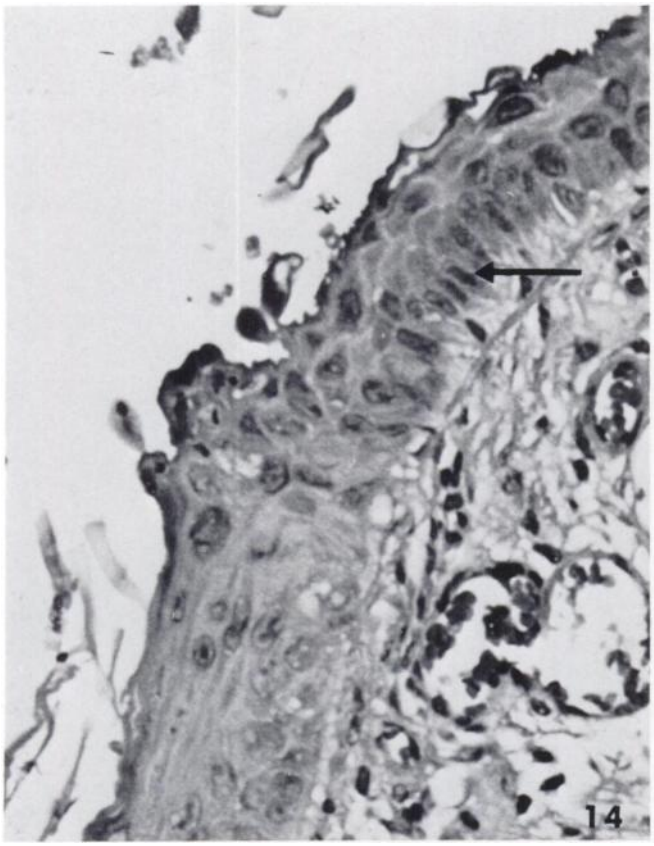

14

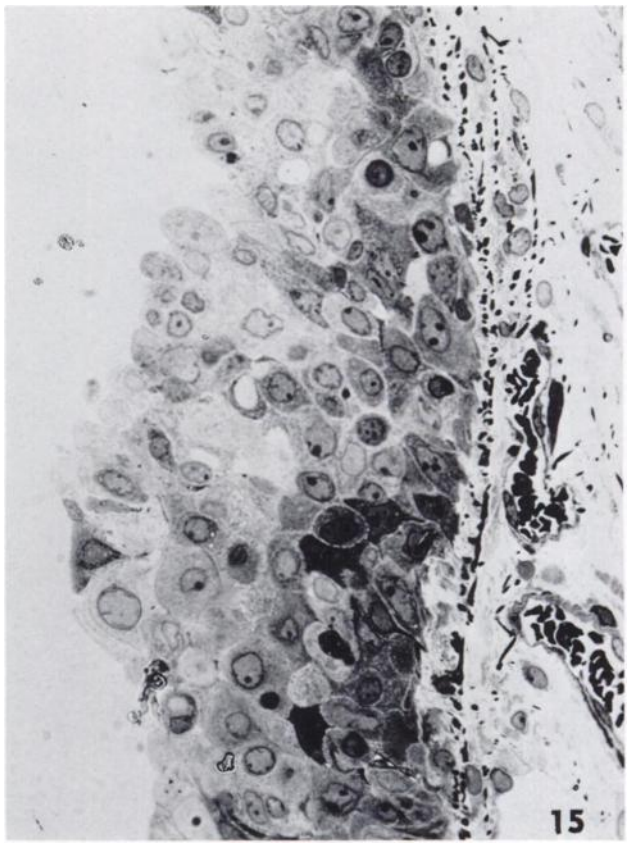

15